

Relationship between natural image statistics and lateral connectivity in the primary visual cortex

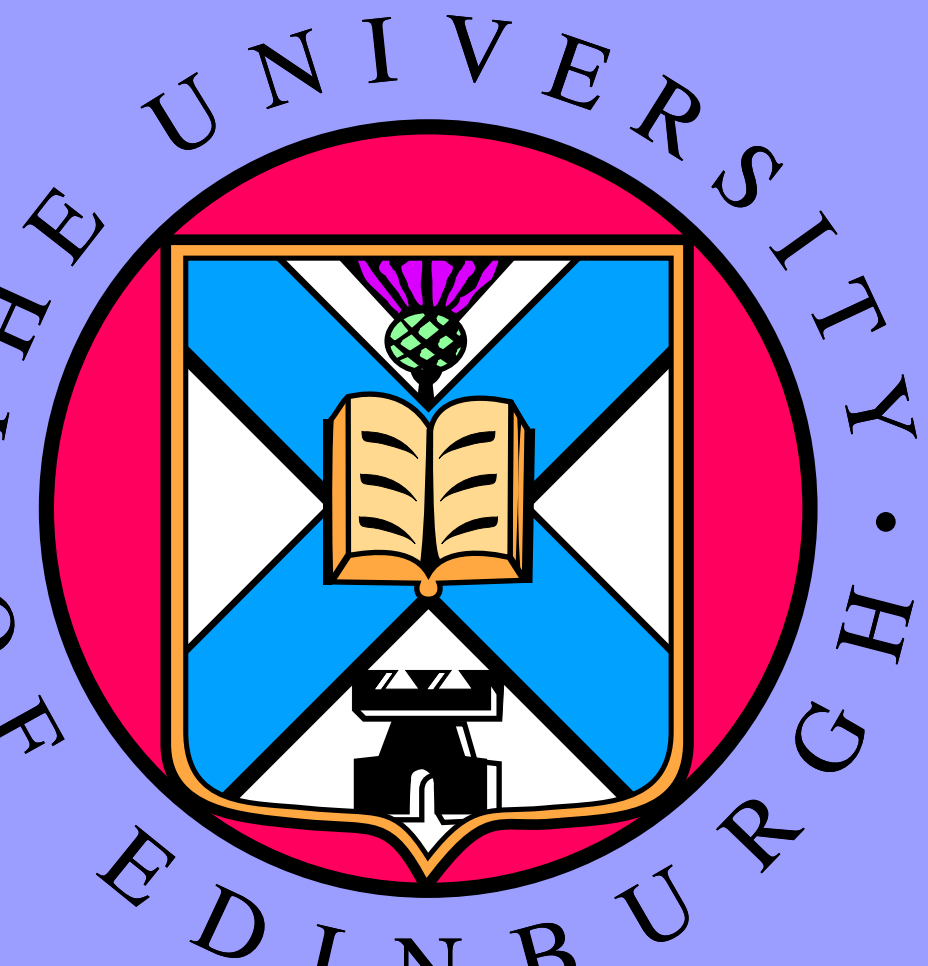
Philipp J. F. Rudiger¹, Jean-Luc Stevens¹, Bharat Talluri¹
 Laurent Perrinet² and James A. Bednar¹ Contact: P.Rudiger@ed.ac.uk

1 - Institute of Adaptive and Neural Computation, University of Edinburgh, Edinburgh, UK

2 - Institut de Neurosciences de la Timone, Marseille, France



Doctoral Training Centre
in Neuroinformatics and
Computational Neuroscience



Introduction

The distribution of orientation-selective cells in the primary visual cortex has been found to reflect the first-order statistics of visual inputs, i.e. which orientations are most common during a critical period [1]. Similarly, some properties of the lateral connections between these cells have been found to reflect the second-order statistics of images, i.e. the cooccurrence statistics of oriented edge elements, but the results have differed by species. Specifically, horizontal connections have been found to be elongated along the axis of preferred orientation in tree shrew [2] and owl monkey [3], but not in macaque [4]. It is unclear whether these results indicate genuine species differences, or perhaps differences in the visual environments in which these animals were raised.

Here we analyse the effect of input statistics on lateral excitatory connectivity in a developmental model of primary visual cortex, by relating differences in co-occurrence statistics of distinct image datasets, analysed using methods presented in [5], to corresponding differences in the emergent long-range lateral structure. The goal is to propose a testable series of mechanisms linking visual inputs, to cortical structure, and then to predicted behavioral results on tests of surround modulation.

The model, based on earlier variations of a self-organizing map model, develops robust yet adaptive orientation maps [6], long-range lateral connectivity, and a wide range of contextual modulatory effects in a spatially calibrated circuit of macaque V1 [7]. By training the model using images with previously characterized second-order statistics, we demonstrate that the co-occurrence of oriented edges is encoded within the horizontal connectivity of our model. On that basis we predict patterns of lateral connectivity for animals reared in different environments, which can be tested by in future experiments.

Model Structure

- Visual patterns are presented on the model retina for a simulated saccade.
- Activity is computed as a thresholded dot product propagated to two sheets with ON and OFF center-surround receptive fields.
- Contrast-gain control is mediated via divisive lateral inhibition in the LGN.
- The ON and OFF sheets project to V1 via initially random weight matrices.
- Feedforward activity in excitatory and inhibitory V1 sheets drives interactions until steady-state activity is reached.

[LGN & V1: γ : projection strength, η : neural activity, W : weights, σ : threshold function, C: constant]

$$\text{Activity: } \eta_j(t + \delta t) = \sigma \left(\frac{\sum_p \gamma_p \sum_{i \in F_{jp}} \eta_i(t) \omega_{ij}}{c + \gamma_{gc} \sum_{i \in F_{jp}} \eta_i(t) \omega_{ij}} \right)$$

Self-organization is mediated by Hebbian learning, which adjusts connection weights after every saccade. The weights are constrained with divisive post-synaptic weight normalization per projection p with learning rate α_p .

Hebbian Learning: $\omega_{ij}(t + \delta t) = \frac{\omega_{ij}(t) + \alpha_p \eta_j \eta_i}{\sum_{k \in F_{jp}} \omega_{kj}(t) + \alpha_p \eta_j \eta_k}$

The large spatial profile of divisive Pv-ir neurons causes weakly tuned response profiles, while Som-ir neurons develop strong orientation tuning due to their smaller integration area and lower average firing rates.

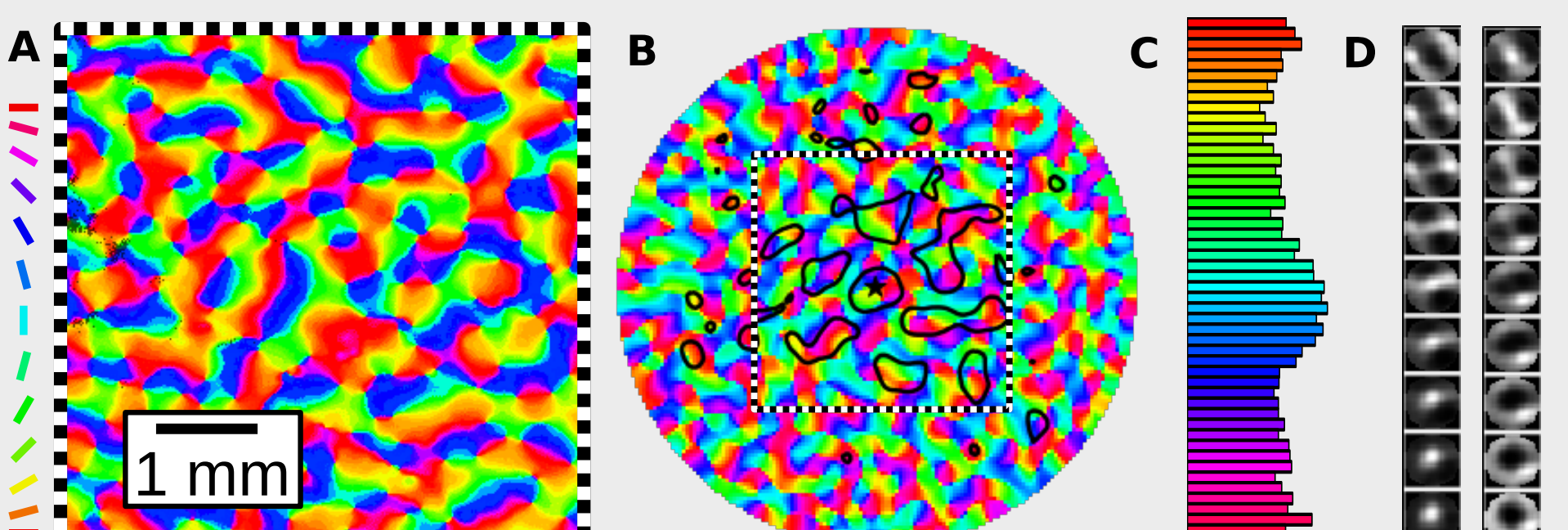
The joint input of Som+ neurons and long-range lateral excitatory connections to excitatory neurons determines the sign and strength of surround modulation.

Methods & Analysis

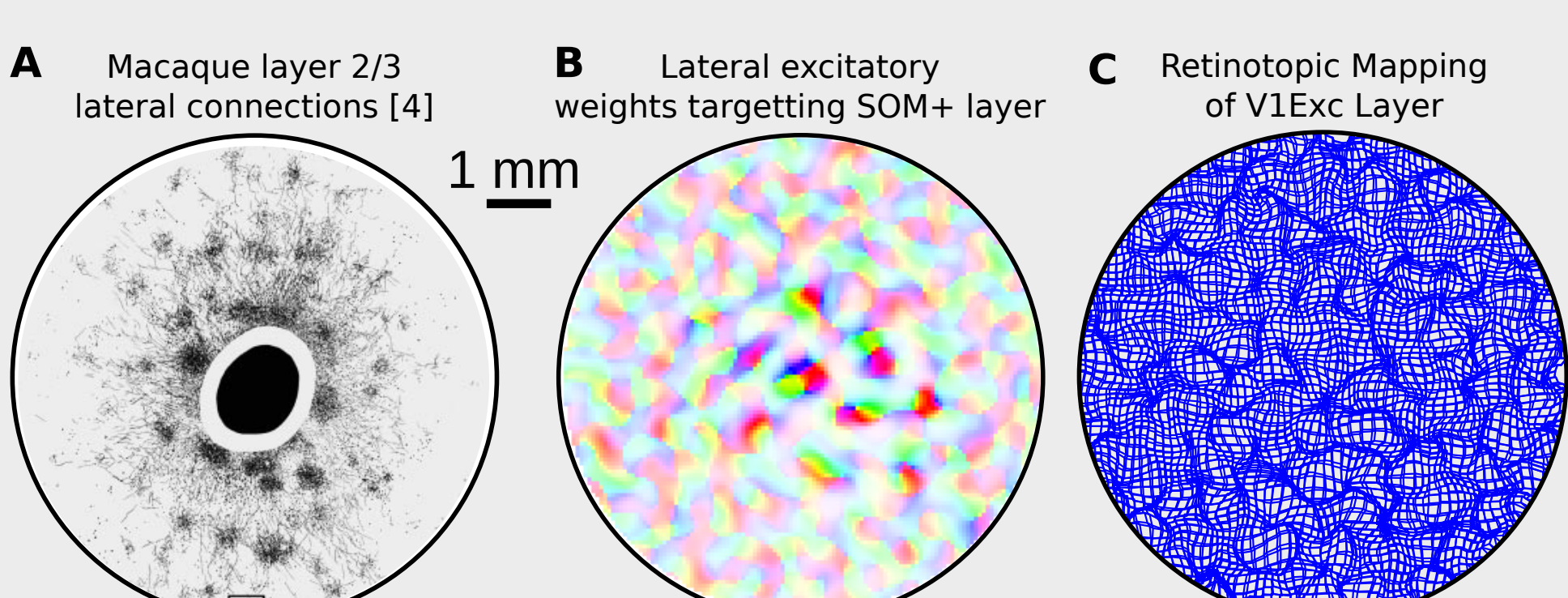


The three datasets analysed for edge co-occurrences used to train the model. A, B) Natural and animal dataset taken from Serre et al. (2007). C) Laboratory dataset.

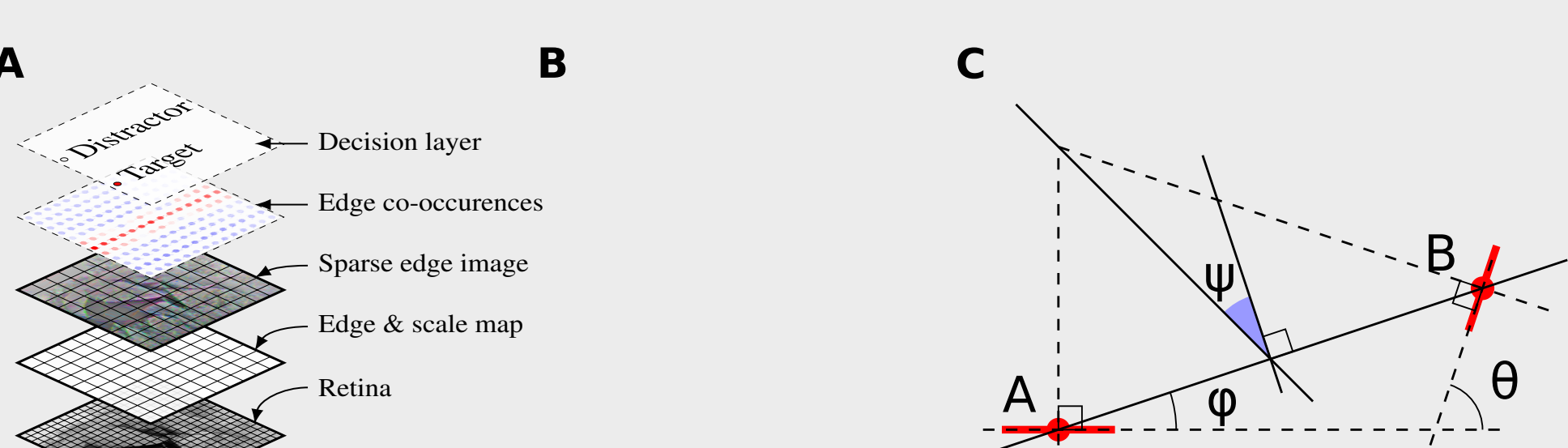
The developmental model presented is independently trained on the three image datasets shown above. From each simulation, the afferent and horizontal model weights were analyzed together with the V1 orientation preference map. A proxy for the cortical retinotopic mapping was derived from the center of gravity of the afferent weights.



A) Orientation map measured in macaque V1 by Blasdel et al. (1992) [8] and B) measured in the spatially calibrated model (black/white box for scale comparison). c) Histogram showing the orientation preference distribution for the orientation map. d) Fully developed LGN Afferent On/Off weights.



A) Lateral connections in macaque V1 layer 2/3 stained using anterograde CTB tracer by Angelucci et al. (2002) [4]. B) Lateral excitatory weight fields as developed over 20,000 image presentations, colored by source orientation preference. C) Retinotopic mapping of V1 excitatory layer.

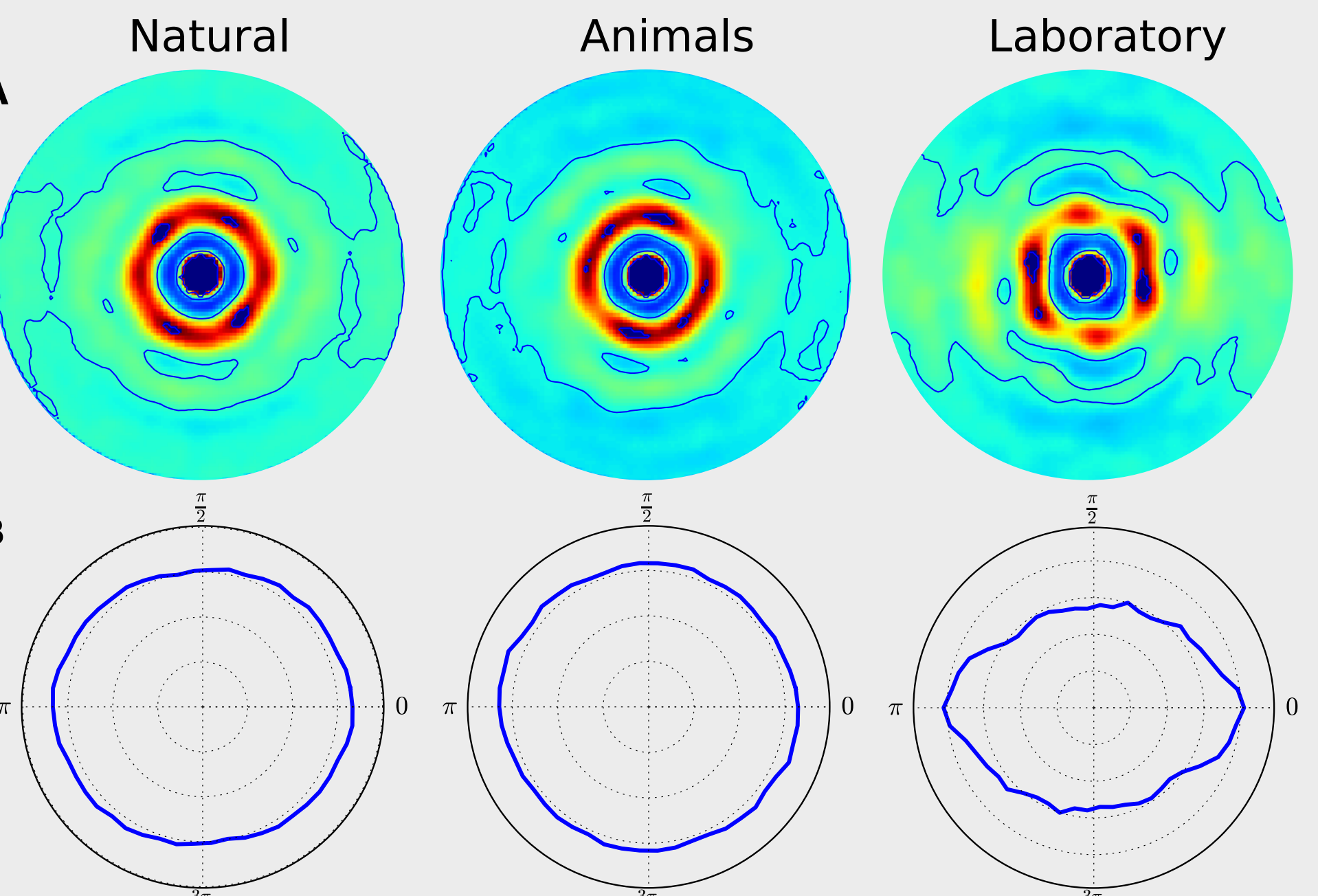


A) Perrinet and Bednar analysed the same datasets used here by finding a sparse set of edges of various spatial frequencies and orientations (e.g. B). This data was used to compute edge co-occurrence statistics by determining the angle θ , ϕ and ψ (defined in C) as well as distance and scale ratio between all pairs of edges. Finally a SVM classifier was used to determine which dataset a particular image belonged to, demonstrating that images could be classified based on their second order statistics alone.

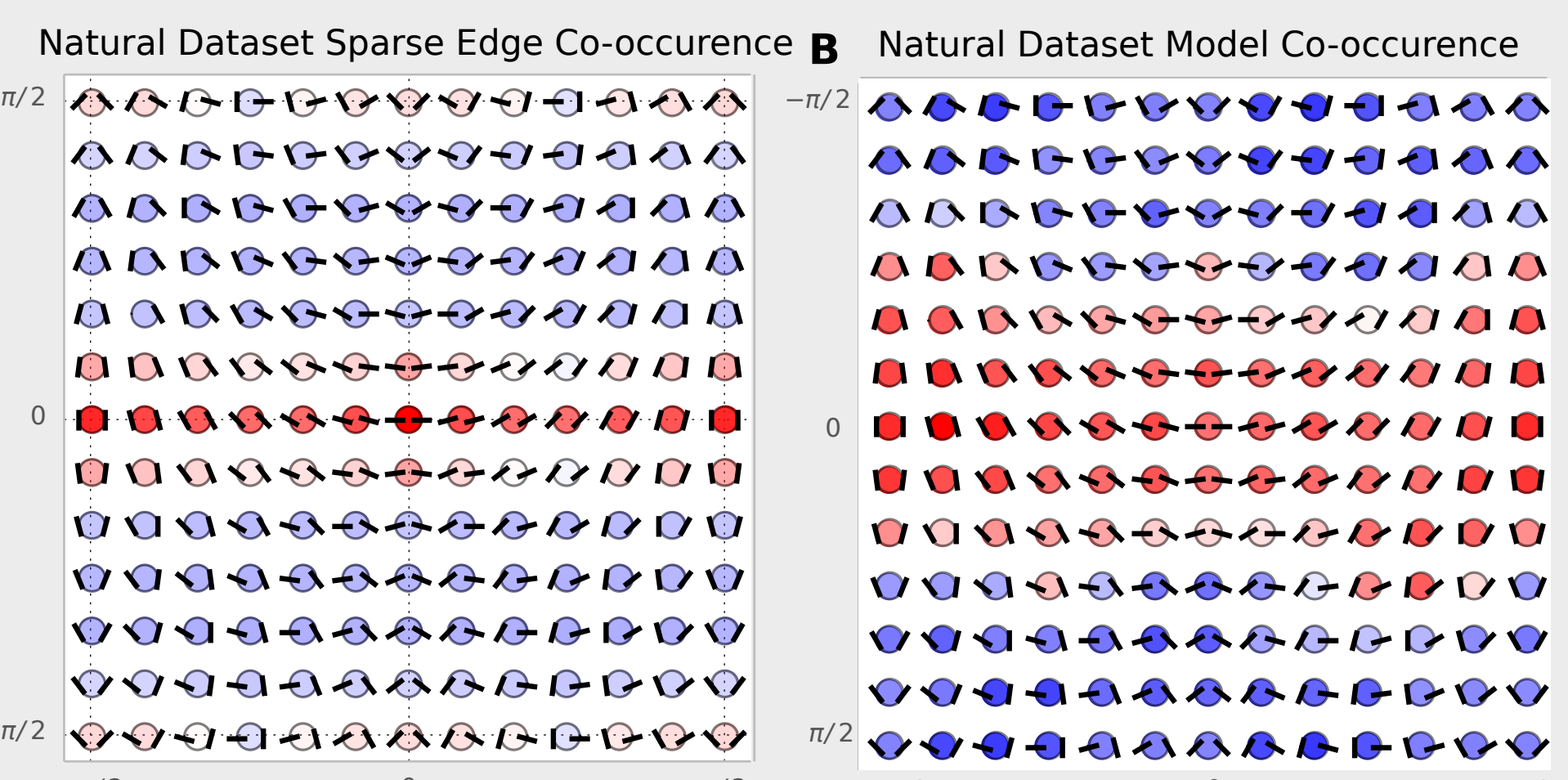
Using the methods for analyzing and visualizing edge co-occurrences developed by Geisler et al. (2001) [9] and extended by Perrinet & Bednar (2014) [5], we extracted the edge co-occurrences encoded within the lateral connections. This was done by iterating over a set of lateral weight fields, finding the orientation difference between each source and target neuron within them to determine the angle θ . The azimuth difference from the source and target retinotopic location, was computed the same way as described in the figure C above.

Results

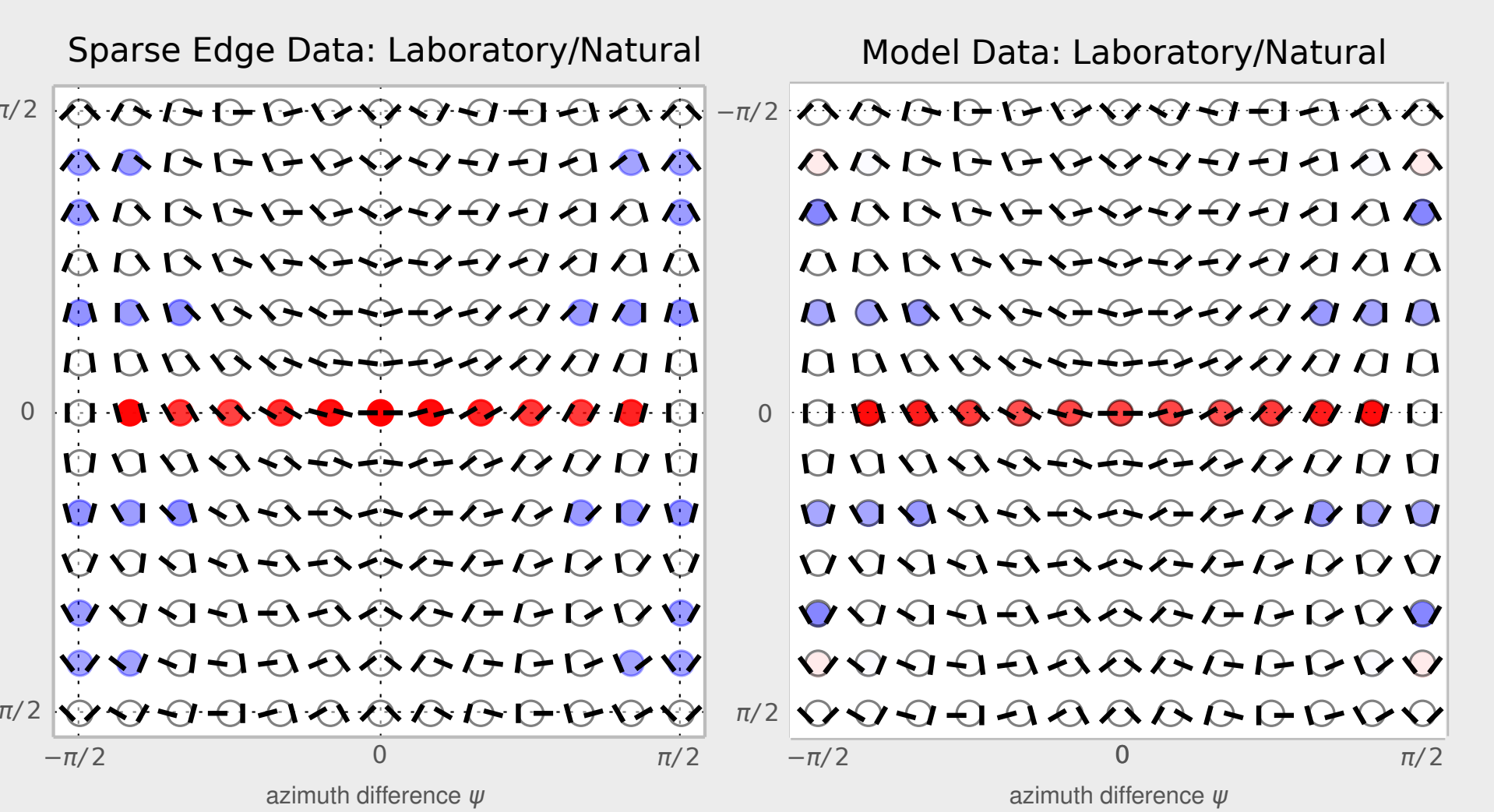
The averaged lateral weights after adjusting for preferred orientation show clear differences in isotropy when comparing the three datasets. The largest amount of anisotropy was found in the laboratory dataset, followed by the natural images, while the animal dataset was almost isotropic.



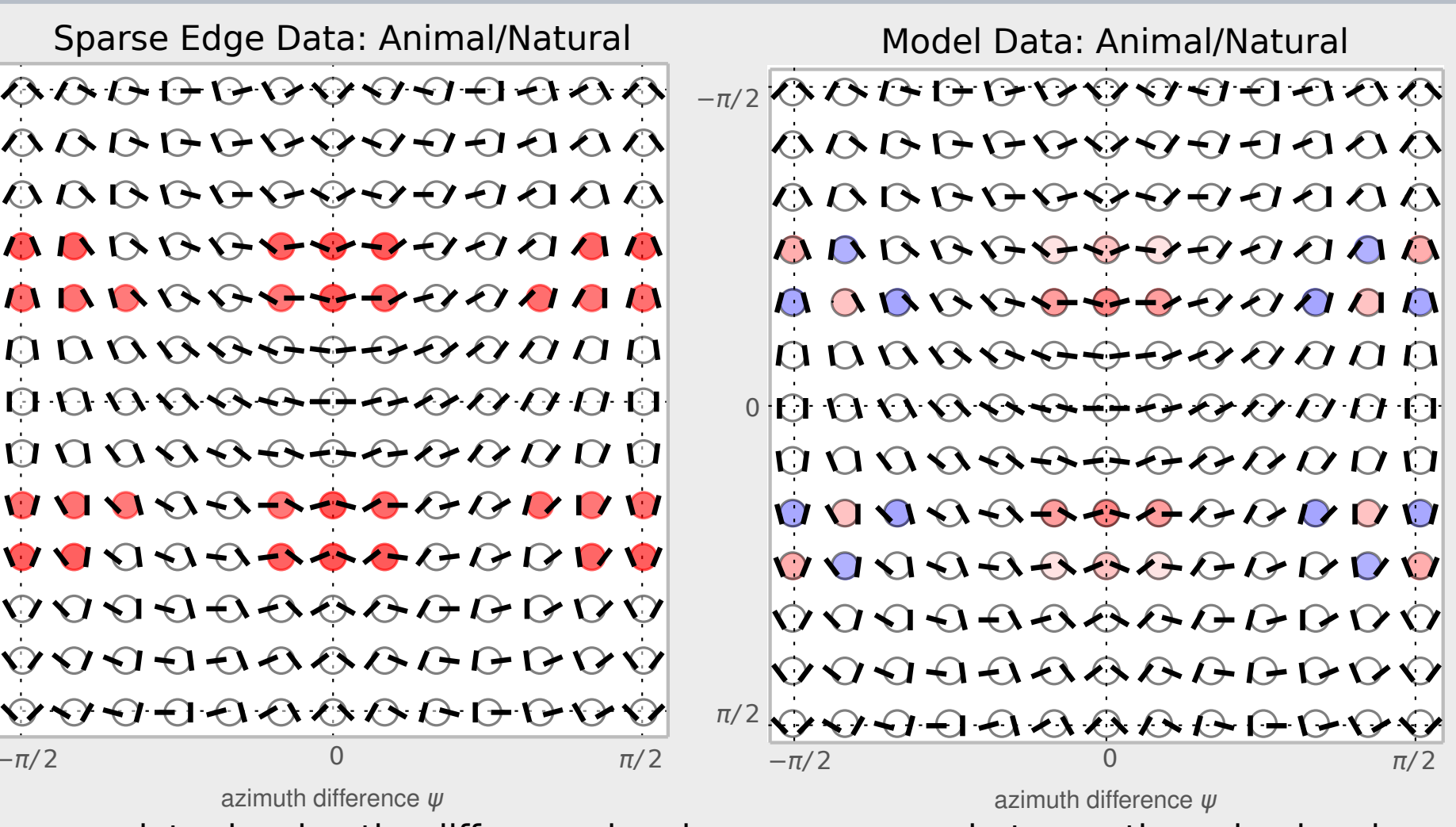
A) Mean lateral weight plots for each dataset, averaged over lateral weight fields rotated to the horizontal relative to the orientation preference of the source neuron. B) Polar plots showing total weight at each azimuth relative to the preferred orientation of the source neuron. Although the natural and animal datasets result in similar levels of anisotropy, i.e., largely isotropic, the laboratory condition shows clear anisotropy along the axis of preferred



A) Cooccurrence chevron maps showing the distribution of different geometric edge configurations generated by analysing the natural image dataset using sparse edge detection algorithm directly. B) Corresponding chevron plot extracted from the lateral connections of the model. Deeper reds indicate higher probabilities and deeper blues lower probabilities. Both plots show a preference for cooccurrence of edges with similar orientation, largely independent of azimuth difference.



A) Chevron maps showing the probability of edge cooccurrence in the laboratory dataset relative to the natural dataset generated from the sparse labelled edges and B) extracted from the model. To highlight the differences, the 32 features with the highest discriminability obtained from the SVM classifier, are shown. The sparse edge data and model data have very high overlap, indicating that lateral weights accurately encode edge cooccurrences.



Chevron plots showing the difference in edge cooccurrence between the animal and natural dataset. Although the similarity is less striking than in the laboratory vs. natural condition, it is clear that the model has captured different cooccurrence statistics between the two datasets.

The results shown here make specific and testable predictions about the effects of visual input statistics on lateral connectivity in primary visual cortex, which can be extended to any set of visual inputs.

Discussion & Conclusion

Here we have shown using our spatially calibrated, developmental model:

- Input statistics can strongly affect the isotropy of lateral connections
- Long-range lateral connections in the model encode the edge cooccurrence statistics of the training inputs.

The approach used to decode the co-occurrence statistics here has several weaknesses primarily because the azimuth calculations are sensitive to the retinotopic location of an afferent receptive field, which was simply determined by finding the center of gravity of the afferent weights.

The work by Perrinet & Bednar [5] that this work builds upon demonstrated that the cooccurrence statistics of edges in natural images are sufficient to classify images as belonging to an animal or distractor dataset with performance rivaling much more complex hierarchical models. This work extends this hypothesis to a mechanistic model of V1, showing that lateral connectivity may encode these statistics and that processing of different image statistics may begin very early in the visual pathway.

Future work will focus on relating the structure of the lateral connectivity to surround modulation effects to investigate the relationship between the learned visual statistics and cortical computation. This work also emphasizes the importance of carefully controlling the rearing environment of animal experimental subjects, may help explain the conflicting observations of lateral connectivity structure in different species and allows us to make testable predictions about the effect of visual experience on lateral structure and surround modulation effects.

References

- Shigeru Tanaka, Jerome Ribot, Kazuyuki Imamura, and Toshiaki Tani. Orientation-restricted continuous visual exposure induces marked reorganization of orientation maps in early life. *NeuroImage*, 30(2):462–77, April 2006.
- W H Bosking, Y Zhang, B Schofield, and D Fitzpatrick. Orientation selectivity and the arrangement of horizontal connections in tree shrew striate cortex. *The Journal of Neuroscience*, 17(6):2112–27, March 1997.
- Philipp Rudiger and James A. Bednar. Unifying anatomical, psychophysical and developmental circuit models of primary visual cortex. In *Society for Neuroscience, page Program No. 639.11/EE10*, 2013.
- L C Sincich and G G Blasdel. Oriented axon projections in primary visual cortex of the monkey. *The Journal of Neuroscience*, 21(8):4416–26, June 2001.
- Alessandra Angelucci, Jonathan B Levitt, Emma J S Walton, Jean-Michel Hupé, Jean Bullier, and Jennifer S Lund. Circuits for local and global signal integration in primary visual cortex. *The Journal of Neuroscience*, 22(19):8633–46, October 2002.
- Laurent Perrinet and James A. Bednar. Edge co-occurrences are sufficient to categorize natural versus animal images. Submitted.
- Jean-luc Stevens, Judith S Law, Jan Antolik, and James A Bednar. Mechanisms for stable, robust, and adaptive development of orientation maps in early life. *Journal of Neuroscience*, 33(40):15747–15766, 2013.
- W Geisler, Y Zhang, B Super, and D Gallopy. Edge co-occurrence in natural images predicts contour grouping performance. *Vision Res*, 41(6):711–724, 2001.
- G Blasdel. Orientation Selectivity, Striate Cortex Preference, and Continuity in Monkey Striate Cortex. *Journal of Neuroscience*, 12(8):3139–3161, 1992.
- W Geisler, J Perry, B Super, and D Gallopy. Edge co-occurrence in natural images predicts contour grouping performance. *Vision Res*, 41(6):711–724, 2001.
- Laurent Perrinet and James A. Bednar. Edge co-occurrences are sufficient to categorize natural versus animal images. Submitted.

This work has made use of the resources provided by the Edinburgh Compute and Data Facility (ECDF). The ECDF is partially supported by the eIDT initiative (<http://www.edikt.org.uk>).